Life Sciences 221 (2019) 35–46

Contents lists available at ScienceDirect

Life Sciences

journal homepage: www.elsevier.com/locate/lifescie

Panaxadiol inhibits synaptic dysfunction in Alzheimer's disease and targets the Fyn protein in APP/PS1 mice and APP-SH-SY5Y cells

Xicai Liang[1], Yingjia Yao[1], Ying Lin, Liang Kong, Honghe Xiao, Yue Shi, Jingxian Yang*

School of Pharmacy, Liaoning University of Traditional Chinese Medicine, Dalian 116600, China

ARTICLE INFO

Keywords:
Alzheimer's disease
Synaptic damage
Panaxadiol
Fyn
Ca^{2+}

ABSTRACT

Aim: Alzheimer's disease (AD), a neurodegenerative disease, is characterized by memory loss and synaptic damage. Up to now, there are limited drugs to cure or delay the state of this illness. Recently, the Fyn tyrosine kinase is implicated in AD pathology triggered by synaptic damage. Thus, Fyn inhibition may prevent or delay the AD progression. Therefore, in this paper, we investigated whether Panaxadiol could decrease synaptic damage in AD and the underlying mechanism.

Main methods: The ability of learning and memory of mice has detected by Morris Water Maze. The pathological changes detected by H&E staining and Nissl staining. The percentage of cell apoptosis and the calcium concentration were detected by Flow Cytometry in vitro. The amount of synaptic protein and related proteins in the Fyn/GluN2B/CaMKIIα signaling pathway were detected by Western Blot.

Key findings: In the present article, Panaxadiol could significantly improve the ability of learning and memory of mice and reduce its synaptic dysfunction. Panaxadiol could down-regulate GluN2B's phosphorylation level by inhibition Fyn kinase activity, Subsequently, decrease Ca^{2+}-mediated synaptic damage, reducing LDH leakage, inhibiting apoptosis in AD, resulting in facilitating the cells survival. For the underlying molecular mechanism, we used PP2 to block the Fyn/GluN2B/CaMKIIα signaling pathway. The results from WB showed that the expression of related proteins in the Fyn signaling pathway decreased with PP2 treated.

Significance: Our results indicate that Panaxadiol could decrease synaptic damage, which will cause AD via inhibition of the Fyn/GluN2B/CaMKIIα signaling pathway. Thus, the Panaxadiol is a best promising candidate to test as a potential therapy for AD.

1. Introduction

Alzheimer's disease, a common degenerative disease, characterized by the aggregation and deposition of amyloid-β (Aβ) and tau. The two key proteins involve had estimated some years before the onset of cognitive impairment [1–5]. Synaptic dysfunction is an early and prominent pathologic feature of AD that frank neuronal loss in AD mice brain [6,7]. A large number of study shows that cortical synaptic density is reduced by 25% to 30% and synaptic density is reduced by 15% to 35% per neuron in even the earliest symptomatic stages of the disease Presynaptic, synaptic, and postsynaptic protein expression levels are reduced in postmortem AD brains compared with controls [8–11]. Thus, synapses became one of the targets in the early intervention of AD. *N*-methyl D-aspartate receptor subtype 2B (NMDAR2B or GluN2B) is the primary NMDARs subunits in the hippocampus. GluN2B is highly permeable to Ca^{2+}, which is essential for excitatory neurotransmission and synaptic plasticity in the nervous system [12–14]. When Fyn phosphorylated at Tyr 416, it can increase phosphorylation of GluN2B at Tyr 1472, thus enhancing Ca^{2+} influx [15–18]. Eventually leads to the exacerbate synaptic dysfunction in AD. However, a little-drugs relieve AD symptoms and have deleterious side effects. Therefore, there is an urgent need for an effective therapeutic agent for AD.

Fyn the Src family of non-receptor tyrosine kinases, play an important role in synapse development and synaptic plasticity. There are multiple lines of evidence linking Fyn kinase function to synapse plasticity and dysfunction in AD [19–21]. In-depth coverage of synaptic loss by Fyn in AD has previously been reported. Increasing neuronal expression of Fyn in human Aβ-forming amyloid precursor protein (APP) transgenic mice model, accelerates synaptic and cognitive impairment, whereas synaptic degeneration and memory loss are rescued when Fyn is either depleted or its activity is suppressed in an APP mutant background [20,22,23]. As such, a great deal of focus has been placed on

* Corresponding author.
E-mail address: jingxian.y@yahoo.com (J. Yang).
[1] These authors contributed equally to this work.

https://doi.org/10.1016/j.lfs.2019.02.012
Received 15 December 2018; Received in revised form 2 February 2019; Accepted 4 February 2019
Available online 05 February 2019
0024-3205/

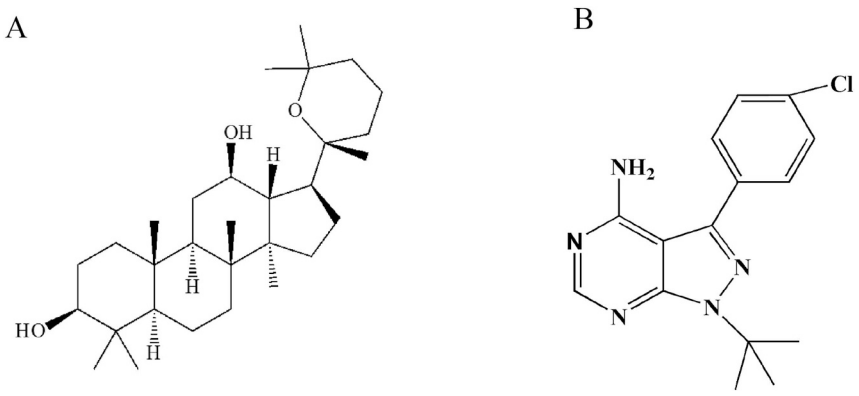

Fig. 1. (A) The chemical structure of Panaxadiol. (B) The chemical structure of PP2.

attempts to understand the mechanisms underlying the structural and functional plasticity of dendritic spines and synapses in AD.

Panaxadiol (Fig. 1) is a triterpenoid saponin monomer compound that is extracted from the roots of *Panax ginseng*. Previous studies have shown that Panaxadiol ameliorates spatial memory impairment and increases the expression of Ach in AD model mice [24,25]. Moreover, the Panaxadiol reduced the death of induced PC12 cells [26,27,28]. But, the studies about whether Panaxadiol can increase the Synaptic protein remained unknown. Therefore, our aimed to investigate the effects of Panaxadiol on the inhibitory of Synaptic damage in treatment for AD and its underlying mechanism. For this purpose, we specifically targeted Fyn specifically in APP/PS1 mice model and APP-SH-SY5Y cells. We found that, activated Fyn/GluN2B/CaMKIIα signaling decrease protein expression of synapsin-1 (SYN) and synaptophysin (SYP), a function that is critical to the released of neurotransmitters. In order to investigate the underlying mechanism, we used PP2 to block Fyn signaling pathway to detect the expression of Synaptic. The results of our study not only provide evidence for the Neuroprotective effects of Panaxadiol to neurological symptoms but also help identify a new therapeutic target for the selective neuropathology of AD.

2. Materials and methods

2.1. Preparation of Panaxadiol and PP2

Panaxadiol (Dammarne-3Beat, $C_{30}H_{52}O_3$, 460.73 Da, the chemical structure as shown in Fig. 1A, > 98% purity) has purchased from the Chengdu Pufei De Biotech Co., Ltd. (Cat. No. 19666-76-3; Chengdu, China), dissolved in 50% PEG-400, and stored in 4 °C.

PP2 (1H-Pyrazolo [3,4-*d*] Pyrimidin-4-amine, 3-(4-chloropheny)-1-(1, 1-dimethylethylethyl), $C_{15}H_{16}C_lN_5$, 301.77 Da, the chemical structure shown in Fig. 1B, > 99.23% purity) has purchased from the MedChem Express (Cat. No. 172889-27-99, USA), dissolved in DMSO, and stored in −80 [29].

2.2. Animal

APP/PS1 double transfected mice have C57BL/6 background and Wild-type (WT) C57BL/6 (9-month-old; body weight 18–22 g), were obtained from the Model Animal Resource Information Platform (SPF, SCXK (J), 2017-0002, SCXK (J), 2017-0008, Nanjing, China). All mice were maintained in a temperature controlled (22 ± 2 °C) environment and in 50–60% of relative humidity for the time period of 12 h in the light, and 12 h in the dark per day during the experiment period. All experimental procedures performed in accordance with the guidelines of the Institutional Animal Care Committee of Liaoning University of Traditional Chinese Medicine (LNUTCM). Cognitive impairment first appears in 7-month-old TG mice, and Aβ deposits in the hippocampus and cortex could be detected in 10-month-old TG mice [30,31]. In the present study, we used mice have the age of nine months only for experiments and they separated randomly into the following three groups normal (WT) group, APP/PS1 (TG) group, (APP/PS1 + PD), (TG + PD) group, each group ten mice. PD administration groups including PD-12.5 mg/kg, PD-25 mg/kg, PD-50 mg/kg groups [32], treated with single dose of Panaxadiol (50% PEG400) by hypodermic injection (i.c.) for six consecutive weeks.

2.3. Morris water maze test

After 5 weeks treatment with Panaxadiol, Morris water maze (Chengdu TME Technology Co., Ltd., Chengdu, China) used to evaluate learning and memory capacity of the mice following the methods which previously described [33]. The apparatus consisted of a circular pool (120 cm diameter × 60 cm height) with a black inner wall, which subdivided into four equal quadrants and filled with water (25 °C) to the depth of 30 cm. An escape platform (10 cm diameter) placed in one of the quadrants (the target quadrant) and submerged 2 cm below the surface of the water. The test contained a platform trial to measure the animal's spatial acquisition ability and a spatial probe test to assessed memory. All the data, including the swim path and the swim time, measured by a camera and automated analyzing system.

2.4. Enzyme-linked immunosorbent assays (ELISA)

After the Morris water maze test, the mice i.c. anaesthetized with 10% chloral hydrate and the whole brain tissue removed and the hippocampal isolated from the brains. Then a part of hippocampal tissues of each mice respectively was made into a 10% cold saline homogenate. Supernatant of the cell homogenate collected and assayed for SYN using an enzyme-linke immunosorbent assay (ELISA) kit (Cat. No.537180424, Tianjin Anoxic Bio-technology CO., Ltd.; Tianjin, China) according to the manufacturer's instruction, and the protein concentration was determined by BCA protein assay kit (Wan lei Bio, Shenyang, China) [28,34].

2.5. HE staining and Nissl staining

Hematoxylin and Eosin (HE) staining used frequently over the years, to examined sections of brain [35,36]. Nissl staining also revealed that the histological method for visualizing neurons in the brain [35,37]. In this study, 4 μm slices for HE and Nissl staining. The sections incubated with reagents according to the staining assays' instructions. The HE and Nissl staining sections visualized on an OLYMPUS SZX9 and BX51 microscope (Tokyo, Japan) with a digital camera.

2.6. Cell culture and APP gene transduction

Human SH-SY5Y cells used throughout the study (Cat. No. CRL-

2266, ATCC). SH-SY5Y cells and human embryonic kidney (HEK293T, Cat. No. 41500034, ATCC) cells cultured in DMEM/F12 supplemented with 10% of fetal bovine serum (FBS), 100 U/mL of penicillin, and 100 μg/mL of streptomycin (all from Gibco, New York, SUA) at 37 °C, 5.0% CO2 with saturated humidity. Then, the lentiviral vectors with $APP_{695/696}$ (Cat. No. EX-A0485-Lv206, GeneCopoeia Biotechnology Co. Ltd. Guangzhou, China) and three helper plasmids, such as pLP1, pLP2 and pLP/VSVG (Cat. No. Z5882, G0125, GeneCopoeia Biotechnology Co. Ltd) fused into HEK 293 T cells [38]. The virus supernatants collected and transfected into the SH-SY5Y cells GFP as a control group. Stably transfected cells screened in the presence of 4 μg/mL puromycin (Cat. No. 53-79-2, Solarbio, Beijing, China). Then we used RT-PCR and Western blot methods to determine the expressions of APP mRNA and protein to confirm whether AD cells model established successfully.

2.7. CCK-8 assay and LDH assay

Cells seeded at a density of 5×10^3 cells per well of 96 well in Complete medium. And the cells viability and release of lactate dehydrogenase measured by CCK-8 assays (Cat. No.CA1210, Solarbio) and LDH assay (Cat. No. BC0685, Solarbio), respectively, according to the manufacturer's instructions. Cells viability expressed as a percentage of viable cells relative to GFP group using a microplate reader (MR-96A, Mindray, Shenzhen, China) on the absorbance at 450 nm [39]. The LDH levels expressed as the percentage of LDH released into the medium relative to the total LDH activity [40].

2.8. Apoptosis assay

The V-APC Apoptosis Analysis kit (Cat. No. AO2001-11P-H, Sungene Biotech Co., Ltd., Tianjin, China) used to detect the apoptosis of each group. The specific operation performed according to the kit instructions. The SH-SY5Y cells collected and rinsed with PBS to adjust the cell density to 1.0×10^5 cells. The budding buffer resuspend cells after the addition of Annexin V-APC and Propidium Iodide. The reaction carried at room temperature for 5 min in the dark, and the apoptosis detected by flow cytometry within 1 h [41].

2.9. Detection of intracellular Ca^{2+} concentration $[Ca^{2+}]_c$

The intracellular concentration of Ca^{2+} measured with Cal-630™AM (Cat. No. 20531, AAT Bioquest, Sunnyvale, CA) [42]. The AD cells seeded overnight at 1×10^5 cells per 2 mL per well in a 6-wall birack wall Bottom costar plate. On the day of the assay, the medium in the plate incubated with the cells overnight (conditioned medium) removed and stored at 37 °C and 5% CO_2. Cal-630™AM dilute1:1000 in medium for final concentration of 2 μM. Now added to the solubilize in DMSO at 2 mM and wells of the plate [43,44]. Dye mixtures incubated with the cells for 60 min in the incubator (37 °C, 5% CO_2). The express of fluorescence intensity detected by flow cytometry.

2.10. RT-PCR analysis of APP mRNA levels

Total RNA extracted using the TRIzol reagent (Invitrogen), and CDNA was synthesized using the Revert Aid First Strand cDNA Synthesis Kit (Fermentas, Lafayette, CO, USA). PCR performed using the DreamTaq Green PCR Master Mix Kit (Thermo Scientific, Lafayette, CO, USA). The APP primers as previously described [35,45] purchased from Guangzhou RiboBio Co, Ltd. (China). The PCR cycling program parameters as follows: 94 °C for 30 s, followed by 35 cycles of 56 °C for 30 s and 72 °C for 1 min and a final extension at 72 °C for 7 min. The PCR products were separated by electrophoresis on 4.0% agarose gels. Quantitative analysis was performed using a Tanon 4100 Gel Imaging System (Tanon Science & Technology Co., Shanghai, China). The RT-PCR primers used in this work as described in Table 1.

2.11. Immunocytochemistry

SH-SY5Y cells grown in 96-well plates fixed in 4% paraformaldehyde for 30 min at 4 °C, washed three times with PBS and permeabilized with 1% Triton X-100 for 5 min at room temperature. Then washed three times with PBS, and incubated with primary antibodies overnight at 4 °C, while the primary antibodies applied: rabbit anti-Fyn (Cat. No. WL01300, Wan lei bio, 1:200), rabbit anti-p-Fyn^{Y416} (Cat. No. AP0511, abclonal, used at 1:200, Wuhan, china), rabbit anti-GluN2B, rabbit anti-p-$GluN2B^{Y1472}$ (Cat. No. bs-3307R, Cat. No. bs-19293R, both Bioss, both used at 1:200, Beijing, china), rabbit anti-Synphilin-1 antibody (Cat. No. ab6179, Abcam, used at, 1:150, Cambridge, MA, USA), cells were washed 3 times in PBS, then incubated for 2 h at RT in either donkey anti-rabbit cy3 (Cat. No. 111-167-003, Jackson Immunol Research Lab, used at 1:400, West Grove, USA) as 50 μL. The cells mounted with a mounting medium (Vector Laboratories, Burlingame, CA, USA) containing DAPI [19,46]. After completion, Photographs has taken with a fluorescence microscope (Nikon Eclipse E600) and the fluorescence intensity measured with Image J 1.38 [47,48].

2.12. Western blotting

The western blotting analysis performed as previously described. Proteins extracted from the hippocampus of each mouse by extraction kit, which contained protease inhibitors methods. Protein concentration determined by the BCA method and 20 μg of protein was resolved by 10% sodium dodecyl sulfate polyacrylamide gel electrophoresis and transferred to a polyvinylidene difluoride (PVDF) membrane, which incubated with primary antibodies followed by appropriate HRP Goat Anti-Rabbit lgG secondary antibodies (Cat. No. AS014, ABclonal, 1:2000). Immunoreactive bands visualized by enhanced chemiluminescence (ECL; Pierce) are scanned on an Image Quant LAS 4000 (GE Healthcare). Image J software used to quantify the optical density of each band [49–51]. The following primary antibodies were used: rabbit anti-Fyn (1:500), rabbit anti-p-Fyn^{Y416} (1:800), rabbit anti-GluN2B (8% SDS, 1:800) and anti-p-$GluN2B^{Y1472}$ (8% SDS, 1:500), rabbit anti-CaMKIIα (Cat. No. WL03064, 1:500, Wanleibio), rabbit Anti-SYP antibody (Cat. No. WL03058, 1:800, Wanleibio), and anti-β-actin (1:2000, Abcam). All the samples coded so that all quantitative analyses could be performed by an observer blinded to the treatment group. Western blot analyses repeated three times and qualitatively similar results obtained.

2.13. Statistical analysis

All data expressed as the mean ± standard deviation (SD) of at least three independent experiments. One-way analysis of variance (ANOVA) with Bonferroni's post hoc test used to evaluate differences among multiple groups. An unpaired two sample Student *t*-test with a confidence interval for the difference between the two groups. GraphPad Prism 5 used and the level of significance was set at $P < 0.05$.

Table 1
The primers for RT-PCR.

Genses	Sense	Anti-sense	Size (bp)
APP	AAAACGAAGTTGAGCCTGTTGAT	GAACCTGGTCGAGTGGTCAGT	350
β-actin	GGGAAATCGTGCGTGACCT	TCAGGAGGAGCAATGATCCTG	385

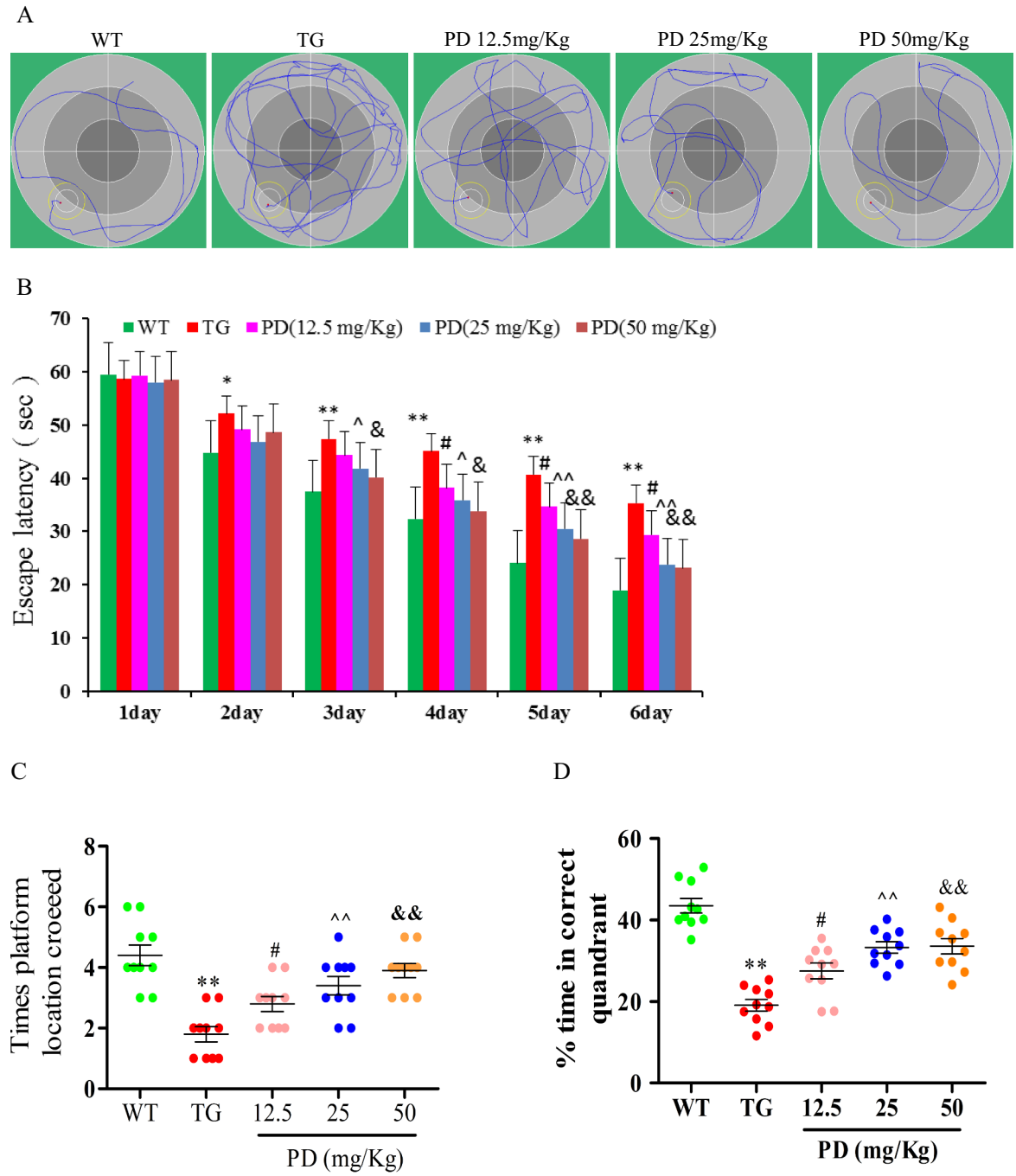

Fig. 2. Effects of Panaxadiol on Cognitive Function of TG Mice.
(A) Representative individual swim paths in the water maze trial (at day 5);
(B) Escape latency in the formal experiments of water maze task;
(C) The number of plat form crossings;
(D) Percentage of time spent in the target quadrant.
Values are expressed as mean ± SD. n = 10, $^{*}P < 0.01$, $^{**}P < 0.01$, $^{\#}P < 0.05$, $^{\#\#}P < 0.01$, $^{\wedge}P < 0.05$, $^{\wedge\wedge}P < 0.05$, $^{\&}P < 0.05$, $^{\&\&}P < 0.01$.

3. Result

3.1. Panaxadiol improves the learning and memory ability of APP/PS1 double TG mice

The learning and memory of APP/PS1 mice evaluated by a Morris water maze test. The experimental results of place navigation (Fig. 2A–B) showed that the TG group significantly prolonged the escape latency compared to the WT group (35.36 ± 2.54 vs. 18.98 ± 5.15 s, $^{**}P < 0.01$), and the Panaxadiol group significantly shortened the escape latency compared to the TG group (F value = 11.07, $^{\#}P < 0.01$, F value = 10.92, $^{\wedge\wedge}P < 0.01$, F value = 13.02, $^{\&\&}P < 0.01$). After the end of the navigation experiment, the platform explored for space experiments to detect the memory capacity of AD mice. The results showed that the TG group significantly decreased the platform crossing times compared to the WT group (1.8 ± 0.51 vs. 4.4 ± 0.8 times, $^{**}P < 0.01$), the Panaxadiol group significantly increased that compared to the TG group (F value = 21.50, $^{\#}P < 0.05$, F value = 19.03, $^{\wedge\wedge}P < 0.01$, F value = 24.59, $^{\&\&}P < 0.01$, Fig. 2C). On the other hand the residence

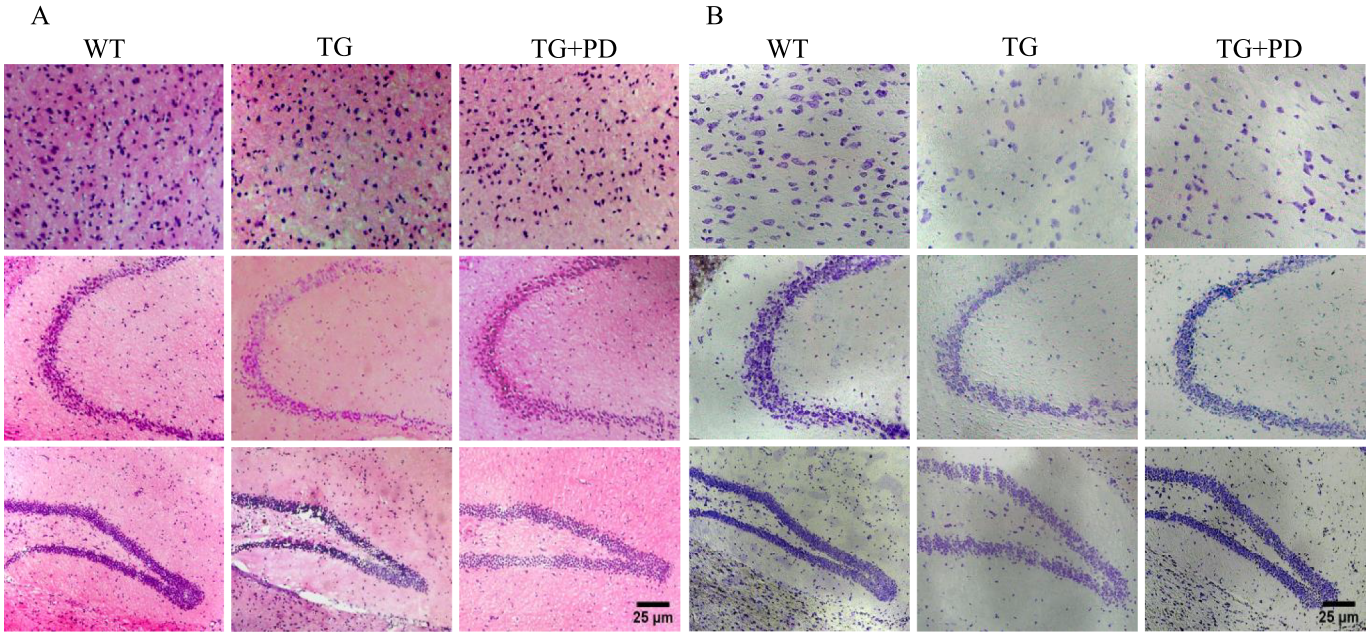

Fig. 3. Panaxadiol reduces the pathological damage of brain tissue in APP/PS1 mice.
(A) Three groups of mice hippocampus and cerebral cortex HE staining;
(B) Three groups of mice hippocampus and cerebral cortex Nissl staining. Scale bar = 25 μm.

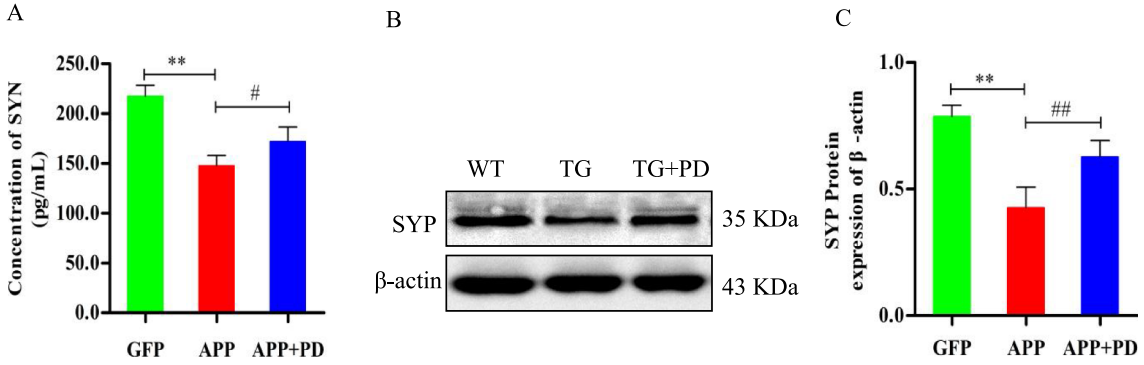

Fig. 4. Effects of Panaxadiol on the SYN expression.
(A) SYN concentrations measured by ELISA assay;
(B) The protien express of SYP was quantitatively analyzed by Western blot;
(C) Quantification of SYP expression, β-actin served as a control.
Datas are expressed as the mean ± SD and represent three independent experiments. $^{*}P < 0.05$, $^{**}P < 0.01$, $^{\#}P < 0.05$, $^{\#\#}P < 0.01$.

time of the quadrant in the WT group was 43.5 ± 4.13 s, and the duration of the quadrant in the TG group was 19.07 ± 3.26 s, ($^{**}P < 0.01$, Fig. 2D) in the TG + PD group were 27.52 ± 4.35, 33.25 ± 3.31 and 33.56 ± 4.51 s in the quadrant of the original platform (F value = 51.55, $^{\#}P < 0.05$; F value = 62.63, $^{\wedge\wedge}P < 0.01$; F value = 51.06, $^{\&\&}P < 0.01$). The above results show that Panaxadiol improved the memory capacity of APP/PS1 double transgenic mice. The concentration of 25 mg/kg Panaxadiol used in the following experiments.

3.2. Panaxadiol ameliorated the histological changes of brains in APP/PS1 mice

H&E and Nissl staining used to observe the histological changes, H&E staining results showed that there were a large number of neuronal cells necrosis and injured neurons with an unclear architecture, nucleus pyknosis in APP/PS1 mice. After Panaxadiol treatment of the damaged ameliorate in hippocampal area (Fig. 3A). Subsequently the results from Nissl staining embedded that the number of neurons significantly reduced in the hippocampal area in APP/PS1 group when treated with Panaxadiol, its cell morphology improved significantly, the number of Nissl increased (Fig. 3B). These results indicated that Panaxadiol could ameliorate the histological changes of brains in APP/PS1 mice.

3.3. Panaxadiol upregulated the concentration of SYP in APP/PS1 mice

We further investigated the effect of Panaxadiol on synapses in APP/PS1 mice, ELISA and Western blot used to analyze the expression of SYN and SYP [3,34]. The results in the present study (Fig. 4A) indicated that the protein levels of SYN significantly decreased in APP/PS1 mice ($^{**}P < 0.01$, compared with WT group), which was significantly reversed by treatment with Panaxadiol in TG group (F value = 25.28, compared with TG group, $^{\#}P < 0.05$). Meanwhile quantitative analysis showed that APP/PS1 mice had a significant decrease in the protein express of SYP, compared with WT group (0.427 ± 0.081% vs.0.787 ± 0.044% $^{**}P < 0.01$ Fig. 4B–C). The protein expresses of SYP had a similar trend of enhanced in TG group with Panaxadiol treated (F value = 23.12, 0.427 ± 0.081%

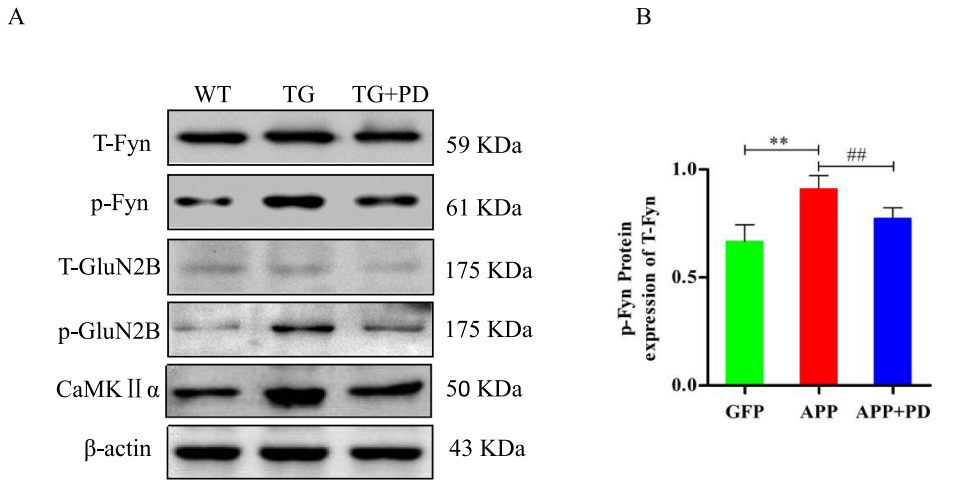

Fig. 5. Effects of Panaxadiol on protein expression in APP/PS1 mice.
(A) Expression of Fyn, GluN2B and CaMKIIα protein in AD mouse detected by western blot;
(B, C) Quantifcation of the levels of p-Fyn^{Y416}, p-GluN2B^{Y1472} and CaMKIIα protein, β-actin served as a control.
(D) Quantifcation of the levels of CaMKIIα protein, β-actin served as a control.
Values are expressed as the mean ± SD and represent three independent experiments. n = 3, $^{*}P < 0.05$, $^{**}P < 0.01$, $^{\#}P < 0.05$, $^{\#\#}P < 0.01$.

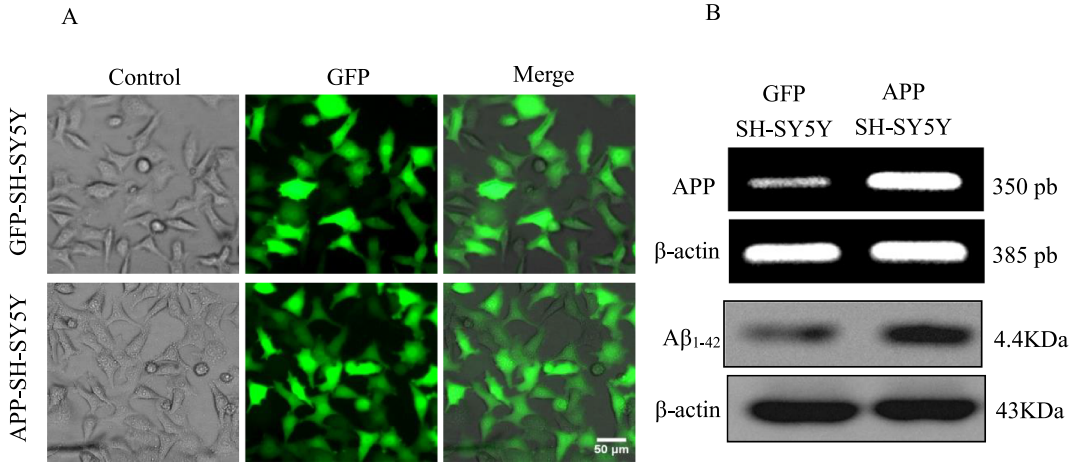

Fig. 6. Transduction of SH-SY5Y cells with a single lentiviral vector encoding APP and GFP.
(A) Lenti-APP-/Lenti-GFP transduced SH-SY5Y cells. Scale bar = 50 μM;
(B) The expression of APP mRNA and protein in GFP and APP-transfected SH-SY5Y cells was detected by RT-PCR and western blot.

vs.0.627 ± 0.065%, $^{\#\#}P < 0.01$, Fig. 4B–C).

3.4. Roles of Panaxadiol in regulating Fyn/GluN2B/CaMKIIα signaling

We examined that the phosphorylation levels of Fyn (Tyr416) and GluN2B (Tyr1472) to investigate the potential involvement of Fyn/GluN2B/CaMKIIα signaling pathway in the Panaxadiol-treated neuroprotection against Synapses damage (Fig. 5A). As shown in Fig. 4B–D the levels of p-Fyn^{Y416}, p-GluN2B^{Y1472} and CaMKIIα protein significantly increased in APP/PS1 group ($^{**}P < 0.01$). However, treatment with Panaxadiol at dose of 25 mg/kg significantly decreased the levels of CaMKIIα, phosphorylated Fyn and GluN2B protein (F value = 10.83, $^{\#\#}P < 0.01$, Fig. 5B; F value = 80.00, $^{\#\#}P < 0.01$, Fig. 5C; F value = 5.107, $^{\#}P < 0.05$, Fig. 5D). As there was no significant difference between total Fyn and GluN2B respectively. These results indicated that Panaxadiol prevented Synapses damage mediated in AD through Fyn/GluN2B/CaMKIIα signaling pathways.

3.5. Transduction of GFP and APP into SH-SY5Y cells

SH-SY5Y cells infected with the two different lentiviral constructs (GFP and APP–GFP). GFP (green) expression observed in cells under

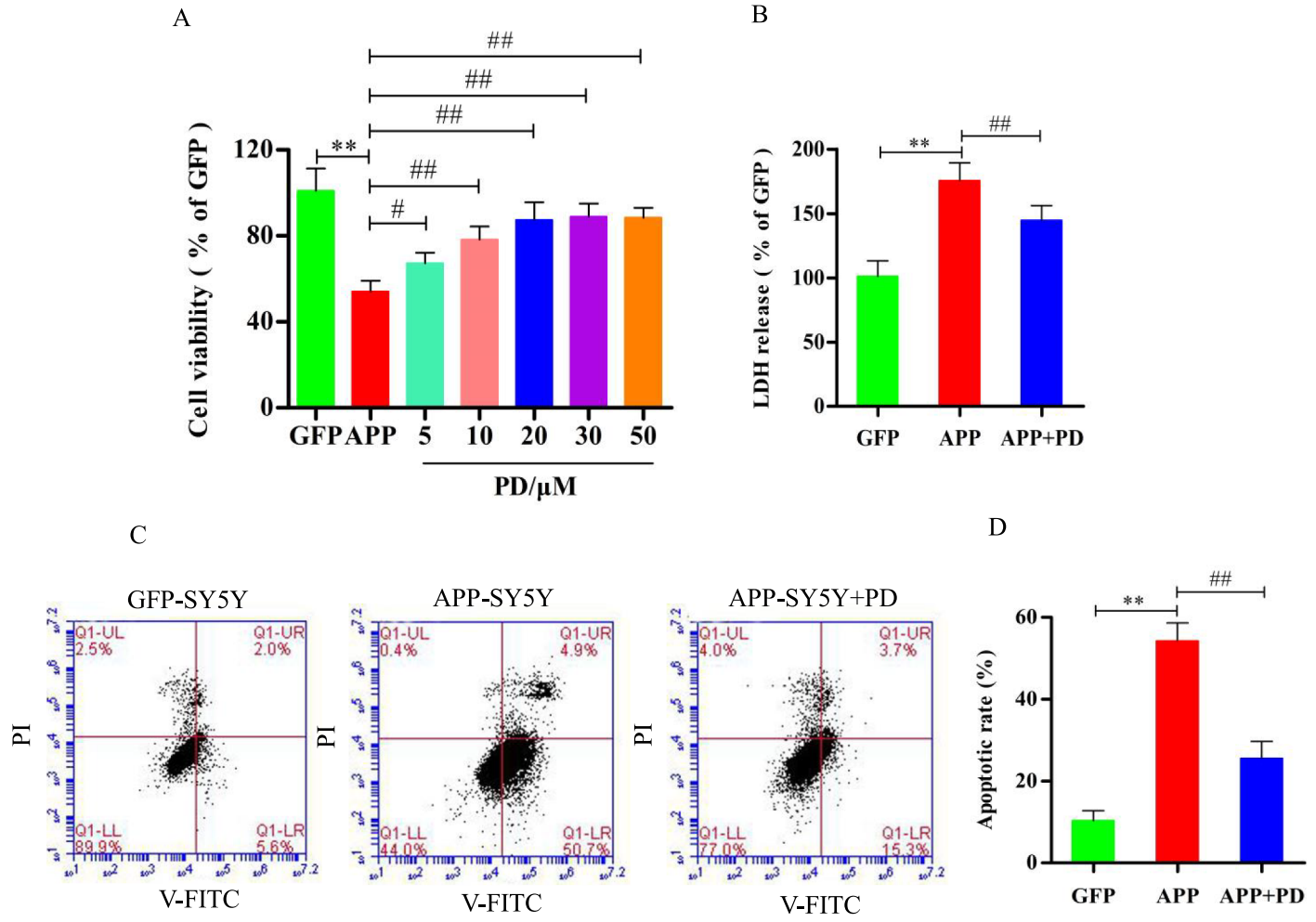

Fig. 7. Panaxadiol suppressed cell damage in SH-SY5Y cells with overexpression of APP.
(A) SH-SY5Y cells overexpressing APPswe were treated with different concentrations of Panaxadiol (0, 5, 10, 20, 30 and 40 μM) for 24 h. Cell viability was determined by CCK-8 assay;
(B) The LDH release in APP-SH-SY5Y cells after the treatment with 20 μM Panaxadiol was measured using LDH assay;
(C) The effects of Panaxadiol on the apoptosis of APP-transfected SH-SY5Y cells were measured by flow cytometry;
(D) Quantitative analysis of apoptosis in SH-SY5Y cells.
The values are expressed as the mean ± SD of three independent experiments. n = 3, $^{*}P < 0.05$, $^{**}P < 0.01$, $^{\#}P < 0.05$, $^{\#\#}P < 0.01$.

fluorescence microscopy (Fig. 6A). The SH-SY5Y cells transduced with lenti–APP–GFP exhibited GFP-positive staining at a rate of 95%. We further investigated the levels of APP mRNA and $A\beta_{1-42}$ protein using RT-PCR and western blot, respectively. The results indicated that the APP mRNA expression significantly increased in the APP-transduced cells. Furthermore, the $A\beta_{1-42}$ protein level was markedly increased by western blots, compared with GFP group (Fig. 6B).

3.6. Neuroprotective effects of Panaxadiol on SH-SY5Y cells transfected with APP

We further investigated that neuroprotective effects of Panaxadiol in AD cells using CCK-8 assay and LDH assay. We further investigated that neuroprotective effects of Panaxadiol in AD cells using CCK-8 assay and LDH assay. Firstly, we detected the effects of Panaxadiol (5, 10, 20, 30, or 40 μM) on the APP-SH-SY5Y cell viability by CCK-8 assay. In Fig. 5A Panaxadiol significantly increased the viability in a dose-dependent manner, and the 20 μM concentration of Panaxadiol restored the cell survival level to 87.43 ± 8.20% vs. APP-SH-SY5Y group (F value = 26.22, $^{\#\#}P < 0.01$). We therefore used this concentration in the next experiments. From the result of LDH assay, we found that the LDH release decreased with Panaxadiol treatment, compared AD cells (F value = 26.75, 144.77 ± 11.56% vs. 175.50 ± 13.80%, $^{\#\#}P < 0.05$, Fig. 5B). These results indicated that Panaxadiol had neuroprotective effects in APP-SH-SY5Y cells.

Next, we determined the cell apoptotic via flow cytometry, which is evaluated using PI marking in the presence of samples extracted using deionized water extracted. The results indicated that cells transduced with APP increased the rate of apoptotic positive cells to 54.26% in GFP-SH-SY5Y ($^{**}P < 0.01$, Fig. 7C–D). Meanwhile, the percentages of apoptotic cells were 25.57 ± 4.05% in APP-SH-SY5Y cells cultured with Panaxadiol (F value = 108.1, $^{\#\#}P < 0.01$, Fig. 7C–D). These results demonstrated that the Panaxadiol could protect the APP-SH-SY5Y cell against apoptosis.

3.7. Panaxadiol increased the express of SYN protein in APP-SH-SY5Y cells via inhibiting Fyn/GluN2B/CaMKIIα signaling pathway

To further investigate the mechanism of Panaxadiol on Synaptic dysfunction, Fyn signaling block used PP2 with 500 nM (Fyn inhibitor), and the levels of Fyn, GluN2B and CaMKIIα were analyzed. As shown in Fig. 8A total Fyn and GluN2B had no significant difference in each group. Interestingly, Aβ significantly increased p-Fyn^{Y416}, p-$GluN2B^{Y1472}$, CaMKIIα protein expressions, which reversed with Panaxadiol treatment (Fig. 8A). The regulation of Panaxadiol on p-Fyn/p-GluN2B/CaMKIIα signaling in APP-SH-SY5Y cells were similar with those in mice model. In order to verify the effects of Panaxadiol on Fyn, we compared the effects of Panaxadiol and above signaling inhibitor. In Fig. 8B Panaxadiol decreased p-Fyn^{Y416}, p-$GluN2B^{Y1472}$ and CaMKIIα protein expression as similar to PP2, and had no significant differences between two groups (p-Fyn: F value = 148.0, $^{\#\#}P < 0.01$; F value = 144.9, $^{\wedge\wedge}P < 0.01$; p-Glun2B: F value = 263.0, $^{\#\#}P < 0.01$; F value = 217.3, $^{\wedge\wedge}P < 0.01$; CaMKIIα: F value = 40.24, $^{\#\#}P < 0.01$, F value = 50.62, $^{\wedge\wedge}P < 0.01$). The results from Immunocytochemistry showed that Synaptic protein were significantly lower in APP-SH-SY5Y cells than in Panaxadiol treated APP-SHSY5Y cells (p-Fyn: F value = 43.20, $^{\#\#}P < 0.01$; F value = 61.09, $^{\wedge\wedge}P < 0.01$; p-Glun2B: F value = 124.8, $^{\#\#}P < 0.01$; F value = 97.66, $^{\wedge\wedge}P < 0.01$; Fig. 8C–D).

There is significant evidence that intracellular Ca^{2+} homeostasis is disrupted in both sporadic and familial forms of AD, and promote Synaptic dysfunction [52]. We therefore, examined the effects of Panaxadiol treatment on intracellular Ca^{2+} concentration in APP -SH-SY5Y cells. We examined whether Panaxadiol could decrease cell Ca^{2+} overload in the APP cells by flow cytometry. According to the number of cells at the same fluorescence intensity showed that APP treatment significantly decreased intracellular peak value of Ca^{2+} (102.33 ± 9.71% vs. 66.37 ± 4.03% in GFP group, $^{**}P < 0.01$, Fig. 8A, B), Panaxadiol and PP2 are restored physiological levels of Ca^{2+} in APP-SH-SY5Y cells (F value = 24.63, $^{\#\#}P < 0.01$; F value = 23.21, $^{\wedge\wedge}P < 0.01$).

Aβ-induced Synaptic damage an important feature of AD could cause apoptosis of the neural cells. It had been shown that damage of Synaptic appears in APP/PS1 mice brain, in this study, we are supposed to detect the expression of SYP and SYN by immunofluorescence assay and WB analysis. In Fig. 8A–D, the results from bands and immunofluorescence intensity of Synaptic protein were significantly lower in APP-SH-SY5Y cells than in Panaxadiol treated APP-SHSY5Y cells (F value = 11.41, $^{\#\#}P < 0.01$, Fig. 8B; F value = 9.233, $^{\#\#}P < 0.01$, Fig. 8D). Further these results in vitro could indicate that Panaxadiol increased the express of SYN protein in APP-SH-SY5Y cells via inhibiting Fyn/GluN2B/CaMKIIα signaling pathway.

4. Discussion

In the present study, we used SH-SY5Y cells stably expressing the Swedish APPswe mutant of human APP as in vitro models and APP/PS1 double TG mice as an in vivo model to investigate the effects of Panaxadiol on APP processing. We found that Panaxadiol significantly inhibited the synaptic damage.

An increasing number of studies suggest that nonreceptor tyrosine kinase Fyn plays a key role in synaptic damage. Strategically located at the postsynaptic density of glutamatergic synapses, it is in an excellent position to modulate the effects of synapses. In AD patient brains, Fyn activities increased. A recent study by Jeannie Chin and colleagues compressed the in synaptic toxicity of high APP and high Fyn. They found that increased the damage of synaptic in the mice expressed with high APP and high Fyn. Inhibiting Fyn activity in neurons rescued memory impairments in TG mice with high levels of APP/PS1 expression and significantly decreased their depletion of synaptic activity-related proteins [15,53–56]. A large number of studies show that Fyn interacted with NMDARs, increased GluN2B-dependent Ca^{2+} influx and increased the damage of synaptic [57,58]. These results highlight the potential significance of pathogenic interactions between APP and Fyn-related signaling pathways.

Panaxadiol, a natural compound with a dammarane skeleton, was extracted from Ginseng [59]. Currently, there were few studies on the Panaxadiol. In this study, we found that the Panaxadiol appear appropriate to achieve Fyn kinase inhibition as a target for AD. Those results showed that Panaxadiol treatment could rescue cells overexpressing APP from neurodegeneration. Including increased the survival rate, mitigated LDH leakage, and neural apoptosis in APP-SH-SY5Y cells, demonstrated neuroprotective action against APP overexpression (Fig. 7). Panaxadiol reduced brain tissue pathological damage in APP/PS1 mice (Fig. 3). To test whether Panaxadiol enhanced the learning and memory function, the Morris water maze test was employed. The results showed that the Panaxadiol stimulation significantly ameliorated the learning and memory deficits of AD mice, which resulted in shortening the escape latency and increasing the time spent in the target zone during the probe test in APP/PS1 double TG mice (Fig. 2A–D).

To elucidate the underlying mechanism of the neuroprotective effects of Panaxadiol, we assessed the influence of Panaxadiol on protein express of SYN and SYP in the AD mice. Synaptic loss is the pathological basis of cognitive deficiency in AD. The protein of SYN and SYP participates in synaptic transmission and can be used to quantify synapses. In this study, we examined the protein expression of SYN and SYP in the AD mice and found that it was downregulated (Fig. 4A–C). After the Panaxadiol treatment, we found that treatment with both doses of Panaxadiol reversed the decreased levels of SYN and SYP in APP/PS1 mice (Fig. 4A–C). The levels of SYN and SYP expression in APP/PS1 mice were consistent with the results of the in vitro experiments (Fig. 8A–E).

To determine the in vivo relevance of the Fyn/GluN2B/CaMKIIα

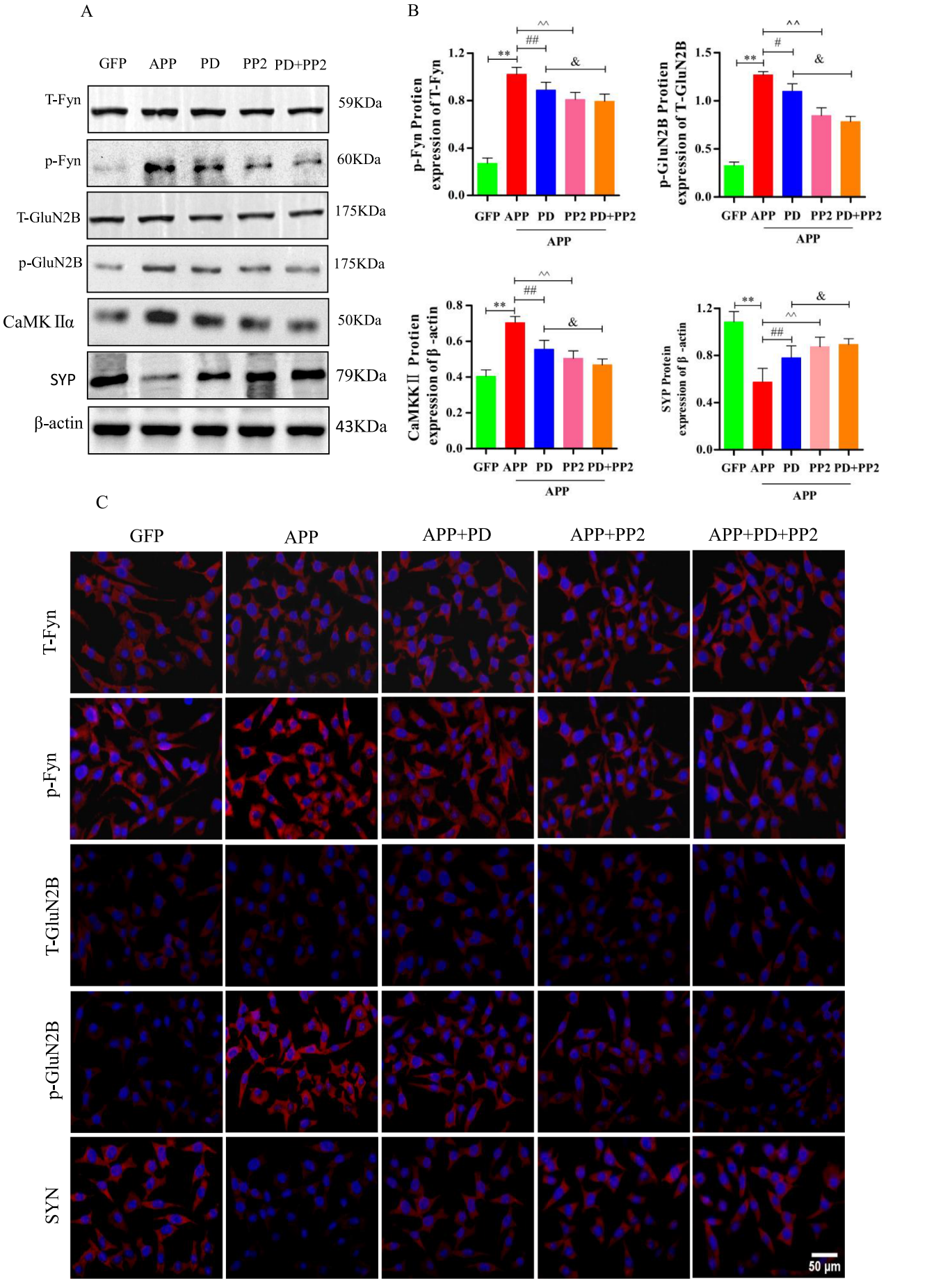

(caption on next page)

Fig. 8. Panaxadiol increased the expressed of SYN via inhibited Fyn/GluN2B signaling pathway.
(A) Expression of Fyn, GluN2B, CaMKIIα and SYP protein in AD mouse detected by western blot;
(B) Quantifcation of the levels of p-Fyn^{Y416}, p-GluN2B^{Y1472}, CaMKIIα and SYP protein, β-actin served as a control.
(C) The levels of Fyn, p-Fyn^{Y416}, GluN2B, p-GluN2B^{Y1472}, SYN proteins were detected by immunocytochemistry assay;
(D) The fluorescence intensity of APP-SH-SY5Y cells were quantified by densitometric measurements;
(E) The $[Ca^{2+}]_c$ in APP-transfected SH-SY5Y cells was measured by flow cytometry;
(F) Quantitative analysis of $[Ca^{2+}]_c$;
The values are expressed as the mean ± SD of three independent experiments. n = 3, $^{**}P < 0.01$, $^{\#}P < 0.05$, $^{\#\#}P < 0.01$, $^{\wedge\wedge}P < 0.01$, $^{\&}P < 0.05$, $^{\&\&}P < 0.01$.

signaling pathway, we explored Aβ-depositing APP/PS1 transgenic mice that overexpress the human amyloid precursor protein (APP) carrying a familial AD mutation. ELISA and Western Blotting confirmed that, compared to WT brains, APP/PS1 brains presented with a pronounced synaptic loss, and in particular, that protein expressed of p-Fyn^{Y416}, p-GluN2B^{Y1472} and CaMKIIα was elevated (Fig. 5). Panaxadiol partially reversed the reduction of synaptic proteins, accompanied by the reduction of p-Fyn^{Y416} and p-GluN2B^{Y1472} and CaMKIIα expressions (Fig. 5B–D). To further validate the downstream role of Fyn/GluN2B/CaMKIIα signaling pathway in neurons, we employed the widely used Fyn inhibitor PP2 to block Fyn/GluN2B/CaMKIIα signaling pathway. In APP-SH-SY5Y cells, Aβ caused significant elevation in synaptic loss,

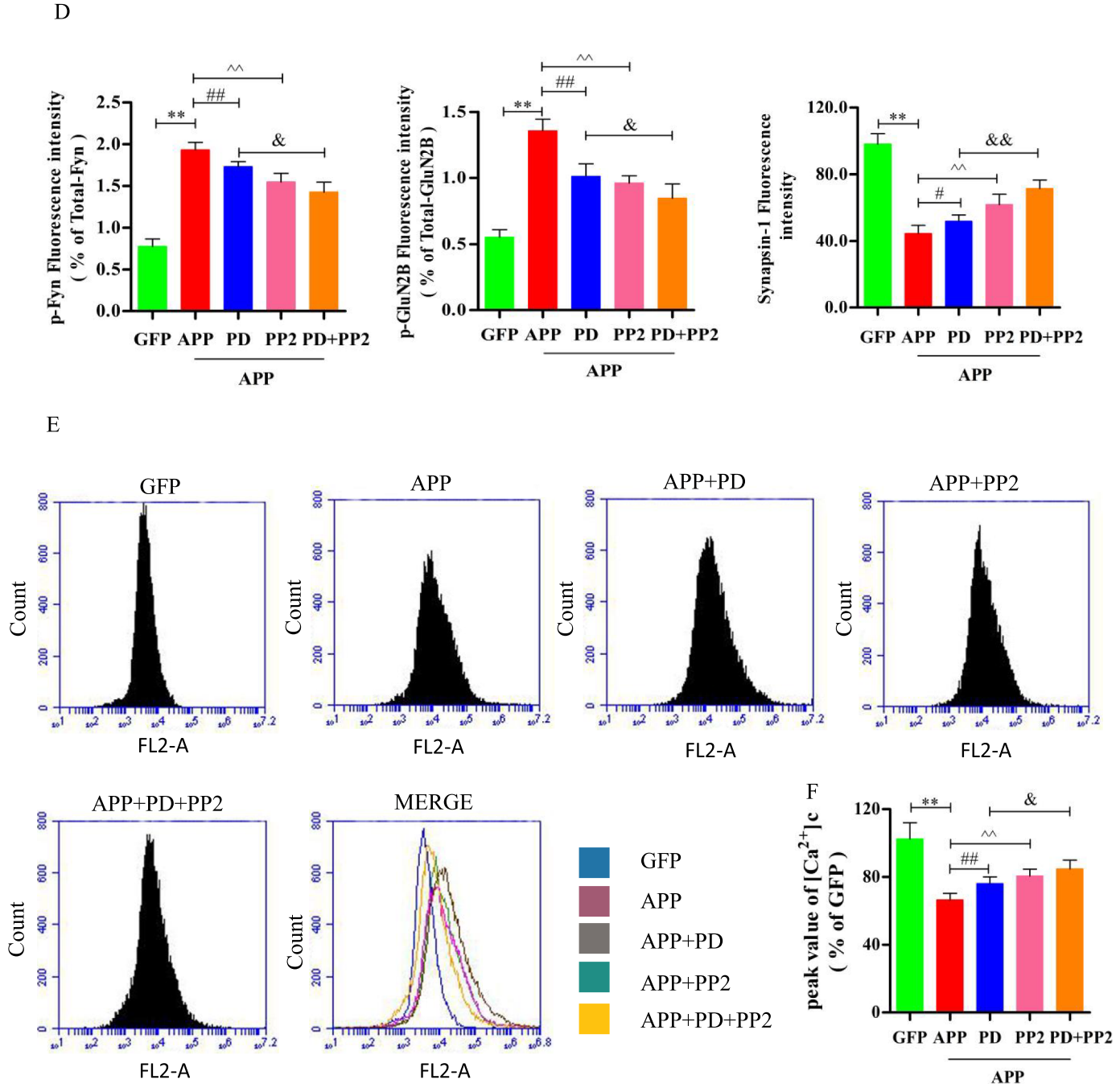

Fig. 8. (*continued*)

together with the more highly activated Fyn/GluN2B/CaMKIIα signaling pathway (Fig. 8A–E). When APP-SH-SY5Y cells were exposed to Panaxadiol and PP2 for 24 h, APP-induced synaptic loss elevation was prevented by Panaxadiol and PP2, as shown by Western blotting. More remarkably, once p-Fyn^{Y416} was blocked by PP2, the downstream p-GluN2B^{Y1472} activation completely disappeared, and mitigated Ca^{2+} overload, suggesting an upstream position of Fyn in regulating GluN2B signaling (Fig. 8B–D). These data indicated that, although APPswe can trigger GluN2B activation independent of Fyn expression, and this Fyn/GluN2B/CaMKIIα activation is because the decreased of synaptic. In summary, this shows that Panaxadiol could suppress the Fyn/GluN2B/CaMKIIα signaling pathway to decrease synaptic loss on AD cells.

In conclusion, our findings revealed that Panaxadiol play a critical role in controlling cell viability, LDH leakage, and apoptosis in cells overexpressing APP. The present results also demonstrated that Panaxadiol increased cell vitality, suppressed LDH leakage, and inhibited cells apoptosis and Ca^{2+} overload, increased synaptic via subsequent downregulation of Fyn/GluN2B/CaMKIIα signaling pathway. In the in vivo study, we also found that Panaxadiol reduced brain tissue pathological damage, inhibit apoptosis, and improve cognitive function. Although the used of Panaxadiol are proposing tactics for the development of Fyn inhibitors. It is important to note that further investigation is required to explore the exact mechanisms by which Panaxadiol regulates Fyn. Thus, Panaxadiol is a promising candidate as a potential therapy for AD.

Competing interests

The authors declare that they have no competing interests. Publisher's Note Springer Nature remains neutral with regard to jurisdictional claims in published maps and institutional affiliations.

Acknowledgments

This work was supported by the National Natural Science Foundation of China (No. 81173580).

Ethics approval and consent to participate

The present study conducted in compliance and accordance with the College of Pharmacy, Liaoning University of Traditional Chinese Medicine and received the necessary ethics approval by the committee.

Consent for publication

Not applicable.

Author contributions

Conceived of the experiment: Jingxian Yang and xicai Liang. Conducted the experiment: xicai Liang. Analyzed the data: Ying Lin, Yue Shi, Liang Kong and Honghe Xiao. Xicai Liang and Yingjia Yao carried out the manuscript preparation. All authors read and approved the final manuscript.

References

[1] T.L. Spires-Jones, The intersection of amyloid beta and tau at synapses in Alzheimer's disease, Neuron 82 (4) (May 2014) 756–771.
[2] H. Kvartsberg, T. Lashley, C.E. Murray, G. Brinkmalm, N.C. Cullen, K. Höglund, H. Zetterberg, K. Blennow, E. Portelius, The intact postsynaptic protein neurogranin is reduced in brain tissue from patients with familial and sporadic Alzheimer's disease, Acta Neuropathol. (Sep) (2018) 22.
[3] S. Sami, N. Williams, L.E. Hughes, T.E. Cope, T. Rittman, I.T.S. Coyle-Gilchrist, R.N. Henson, J.B. Rowe, Neurophysiological signatures of Alzheimer's disease and frontotemporal lobar degeneration: pathology versus phenotype, Brain 141 (8) (Aug 2018) 2500–2510.
[4] E. Nanou, Calcium channels, synaptic plasticity, and neuropsychiatric disease, Neuron 98 (3) (May 2018) 466–481.
[5] R. Kandimalla, M. Manczak, X. Yin, R. Wang, P.H. Reddy, Hippocampal phosphorylated tau induced cognitive decline, dendritic spine loss and mitochondrial abnormalities in a mouse model of Alzheimer's disease, Hum. Mol. Genet. 27 (1) (Oct 2017) 30–40.
[6] J.M. Krivinko, S.L. Erickson, Y. Ding, Z. Sun, P. Penzes, M.L. MacDonald, N.A. Yates, M.D. Ikonomovic, O.L. Lopez, R.A. Sweet, J. Kofler, Synaptic proteome compensation and resilience to psychosis in Alzheimer's disease, Am. J. Psychiatry 175 (10) (Oct 2018) 999–1009.
[7] R. Kandimalla, M. Manczak, D. Fry, Y. Suneetha, H. Sesaki, P.H. Reddy, Reduced dynamin-related protein 1 protects against phosphorylated tau-induced mitochondrial dysfunction and synaptic damage in Alzheimer's disease, Hum. Mol. Genet. 25 (22) (Sep 2016) 4881–4897.
[8] M. Manczak, R. Kandimalla, X. Yin, P.H. Reddy, Hippocampal mutant APP and amyloid beta-induced cognitive decline, dendritic spine loss, defective autophagy, mitophagy and mitochondrial abnormalities in a mouse model of Alzheimer's disease, Hum. Mol. Genet. 27 (8) (Apr 2018) 1332–1342.
[9] M. Manczak, R. Kandimalla, D. Fry, H. Sesaki, P.H. Reddy, Protective effects of reduced dynamin-related protein 1 against amyloid beta-induced mitochondrial dysfunction and synaptic damage in Alzheimer's disease, Hum. Mol. Genet. 25 (23) (Sep 2016) 5148–5166.
[10] W. Gulisano, M. Melone, D.D.L. Puma, M.R. Tropea, A. Palmeri, O. Arancio, The effect of amyloid-β peptide on synaptic plasticity and memory is influenced by different isoforms, concentrations, and aggregation status, Neurobiol. Aging 71 (Nov 2018) 51–60.
[11] C.M. Fernandez-Martos, A.E. King, R.A. Atkinson, A. Woodhouse, J.C. Vickers, Neurofilament light gene deletion exacerbates amyloid, dystrophic neurite, and synaptic pathology in the APP/PS1 transgenic model of Alzheimer's disease, Neurobiol. Aging 36 (Oct 2015) 2757–2767.
[12] E.E. Benarroch, Glutamatergic synaptic plasticity and dysfunction in Alzheimer disease: emerging mechanisms, Neurology 91 (July 2018) 125–132.
[13] J. Wang, X. Lv, Y. Wu, T. Xu, M. Jiao, R. Yang, X. Li, M. Chen, Y. Yan, C. Chen, W. Dong, W. Yang, M. Zhuo, T. Chen, J. Luo, S. Qiu, Postsynaptic RIM1 modulates synaptic function by facilitating membrane delivery of recycling NMDARs in hippocampal neurons, Nat. Commun. 9 (Jun 2018) 2267.
[14] L. Zhu, L. Yang, X. Zhao, D. Liu, X. Guo, Liu Pl, Xanthoceraside modulates NR2B-containing NMDA receptors at synapses and rescues learning-memory deficits in APP/PS1 transgenic mice, Psychopharmacology 235 (1) (Jan 2018) 337–349.
[15] J.W. Um, H.B. Nygaard, J.K. Heiss, M.A. Kostylev, M. Stagi, A. Vortmeyer, T. Wisniewski, E.C. Gunther, S.M. Strittmatter, Alzheimer amyloid-β oligomer bound to postsynaptic prion protein activates Fyn to impair neurons, Nat. Neurosci. 15 (9) (Sep 2012) 1227–1235.
[16] R. Knox, C. Zhao, D. Miguel-Perez, S. Wang, J. Yuan, D. Ferriero, X. Jiang, Enhanced NMDA receptor tyrosine phosphorylation and increased brain injury following neonatal hypoxia–ischemia in mice with neuronal Fyn overexpression, Neurobiol. Dis. 51 (Mar 2013) 113–119.
[17] F. Zhang, A. Guo, C. Liu, M. Comb, B. Hu, Phosphorylation and assembly of glutamate receptors after brain ischemia, Stroke 44 (1) (Jan 2013) 170–176.
[18] E. Yamada, S. Okada, C.C. Bastie, M. Vatish, Y. Nakajima, R. Shibusawa, A. Ozawa, J.E. Pessin, M. Yamada, Fyn phosphorylates AMPK to inhibit AMPK activity and AMP-dependent activation of autophagy, Oncotarget 7 (46) (Nov 2016) 74612–74629.
[19] A.C. Kaufman, S.V. Salazar, L.T. Haas, J. Yang, M.A. Kostylev, A.T. Jeng, S.A. Robinson, E.C. Gunther, C.H. van Dyck, H.B. Nygaard, Fyn inhibition rescues established memory and synapse loss in Alzheimer mice, Ann. Neurol. 77 (6) (Jun 2015) 953–971.
[20] H.B. Nygaard, C.H. van Dyck, S.M. Strittmatter, Fyn kinase inhibition as a novel therapy for Alzheimer's disease, Alzheimers Res. Ther. 6 (1) (Feb 2014) 8.
[21] W. Lu, W. Fang, J. Li, B. Zhang, Q. Yang, X. Yan, Phosphorylation of tyrosine Y1070 at the GluN2B subunit is regulated by synaptic activity and critical for surface expression of NMDA receptors, J. Biol. Chem. 290 (38) (Sep 2015) 22945–22954.
[22] S. Lopes, S.J. Vaz, V. Pinto, C. Dalla, N. Kokras, B. Bedenk, I. Sotiropoulos, Tau protein is essential for stress-induced brain pathology, Proc. Natl. Acad. Sci. U. S. A. 113 (26) (Jun 2016) E3755–E3763.
[23] T.M. Scales, P. Derkinderen, K.Y. Leung, H.L. Byers, M.A. Ward, C. Price, I.N. Bird, T. Perera, S. Kellie, R. Williamson, B.H. Anderton, Tyrosine phosphorylation of tau by the SRC family kinases lck and fyn, Mol. Neurodegener. 6 (Jan 2011) 12.
[24] J.W. Liu, S.J. Tian, J.D. Barry, B. Luu, Panaxadiol glycosides that induce neuronal differentiation in neurosphere stem cells, J. Nat. Prod. 70 (8) (Aug 2007) 1329–1334.
[25] K.H. Kim, D. Lee, Beneficial effects of for the treatment and prevention of neurodegenerative diseases: past findings and future directions, J. Ginseng Res. 42 (3) (Jul 2018) 239–247.
[26] D.H. Bak, H.D. Kim, Y.O. Kim, C.G. Park, S.Y. Han, J.J. Kim, Neuroprotective effects of 20 (S)-protopanaxadiol against glutamate-induced mitochondrial dysfunction in PC12 cells, Int. J. Mol. Med. 37 (2) (Feb 2016) 378–386.
[27] L. Gan, Z.H. Wang, H. Zhang, X. Zhou, H. Zhou, C. Sun, J. Si, R. Zhou, C.J. Ma, J. Li, Endothelium-independent vasorelaxant effect of 20 (S)-protopanaxadiol on isolated rat thoracic aorta, Acta Pharmacol. Sin. 37 (12) (Dec 2016) 1555–1562.
[28] H. Li, T. Kang, B. Qi, L. Kong, Y. Jiao, Y. Cao, J. Zhang, J. Yang, Neuroprotective effects of ginseng protein on PI3K/Akt signaling pathway in the hippocampus of D-galactose/AlCl3 inducing rats model of Alzheimer's disease, J. Ethnopharmacol. 179 (Feb 2016) 162–169.
[29] C. Li, J. Götz, Somatodendritic accumulation of Tau in Alzheimer's disease is promoted by Fyn-mediated local protein translation, EMBO J. 36 (21) (Sep 2017) 3120–3138.

[30] Y. Peng, C. Hou, Z. Yang, C. Li, L. Jia, J. Liu, Y. Tang, L. Shi, Y. Li, J. Long, J. Liu, Hydroxytyrosol mildly improve cognitive function independent of APP processing in APP/PS1 mice, Mol. Nutr. Food Res. 60 (11) (Nov 2016) 2331–2342.
[31] J. Bao, M. Qin, Y.A.R. Mahaman, B. Zhang, F. Huang, K. Zeng, Y. Xia, D. Ke, Q. Wang, R. Liu, J.Z. Wang, K. Ye, X. Wang, BACE1 SUMOylation increases its stability and escalates the protease activity in Alzheimer's disease, Proc. Natl. Acad. Sci. U. S. A. 115 (15) (Apr 2018) 3954–3959.
[32] Chinese Pharmacopoeia Commission, Pharmacopoeia of the People's Republic of China, People's Medical Publishing House, Beijing, 9787506744393, 2015 (ISBN:).
[33] Y. Yao, Y. Wang, L. Kong, Y. Chen, J. Yang, Osthole decreases tau protein phosphorylation via PI3K/AKT/GSK-3β signaling pathway in Alzheimer's disease, Life Sci. 217 (Jan 2019) 16–24.
[34] S. Li, Y. Yan, Y. Jiao, Z. Gao, Y. Xia, L. Kong, Y. Yao, Z. Tao, J. Song, Y. Yan, G. Zhang, J. Yang, Neuroprotective effect of osthole on neuron synapses in an alzheimer's disease cell model via upregulation of microRNA-9, J. Mol. Neurosci. 60 (1) (Sep 2016) 71–81.
[35] J. Song, N. Li, Y. Xia, Z. Gao, S.F. Zou, L. Kong, Y.J. Yao, Y.N. Jiao, Y.H. Yan, S.H. Li, Z.Y. Tao, G. Lian, J.X. Yang, T.G. Kang, Arctigenin treatment protects against brain damage through an anti-inflammatory and anti-apoptotic mechanism after needle insertion, Front. Pharmacol. 7 (Jun 2016) 182.
[36] W.S. Jin, L.L. Shen, X.L. Bu, W.W. Zhang, S.H. Chen, Z.L. Huang, J.X. Xiong, C.Y. Gao, Z. Dong, Y.N. He, Z.A. Hu, H.D. Zhou, W. Song, X.F. Zhou, W.S. Jin, L.L. Shen, X.L. Bu, W.W. Zhang, S.H. Chen, Z.L. Huang, J.X. Xiong, C.Y. Gao, Z. Dong, Y.N. He, Z.A. Hu, H.D. Zhou, W. Song, X.F. Zhou, Peritoneal dialysis reduces amyloid-beta plasma levels in humans and attenuates Alzheimer-associated phenotypes in an APP/PS1 mouse model, Acta Neuropathol. 134 (2) (Aug 2017) 207–220.
[37] Y. Xia, L. Kong, Y. Yao, Y. Jiao, J. Song, Z. Tao, Z. You, J. Yang, Osthole confers neuroprotection against cortical stab wound injury and attenuates secondary brain injury, J. Neuroinflammation 12 (Sep 2015) 155.
[38] J. Yang, Y. Yan, Y. Xia, T. Kang, X. Li, B. Ciric, H. Xu, A. Rostami, G.X. Zhang, Neurotrophin 3 transduction augments remyelinating and immunomodulatory capacity of neural stem cells, Mol. Ther. 22 (2) (Feb 2013) 440–450.
[39] K. Fukuyama, S. Kakio, Y. Nakazawa, K. Kobata, M. Funakoshi-Tago, T. Suzuki, Roasted coffee reduces β-amyloid production by increasing proteasomal β-secretase degradation in human neuroblastoma SH-SY5Y cells, Mol. Nutr. Food Res. 62 (21) (Nov 2018) e1800238.
[40] Y. Liu, H. Wang, M. Yang, N. Liu, Y. Zhao, X. Qi, Y. Niu, T. Sun, Y. Li, J. Yu, Cistanche deserticola polysaccharides protects PC12 cells against OGD/RP-induced injury, Biomed. Pharmacother. 99 (Mar 2018) 671–680.
[41] X. Zheng, Z. Xie, Z. Zhu, Z. Liu, Y. Wang, L. Wei, H. Yang, H. Yang, Y. Liu, J. Bi, Methyllycaconitine alleviates amyloid-β peptides-induced cytotoxicity in SH-SY5Y cells, PLoS One 9 (10) (Oct 2014) e111536.
[42] Y.G. Ma, Y.B. Zhang, Y.G. Bai, Z.J. Dai, L. Liang, M. Liu, H.T. Guan, Berberine alleviates the cerebrovascular contractility in streptozotocin-induced diabetic rats through modulation of intracellular Ca^{2+} handling in smooth muscle cells, Cardiovasc. Diabetol. 15 (1) (Apr 2016) 63.
[43] C. Tischbirek, A. Birkner, H. Jia, B. Sakmann, A. Konnerth, Deep two-photon brain imaging with a red-shifted fluorometric Ca^{2+} indicator, Proc. Natl. Acad. Sci. U. S. A. 112 (36) (Sep 2015) 11377–11382.
[44] H. Qian, Q. Chen, S. Zhang, L. Lu, The claudin family protein FigA mediates Ca^{2+} homeostasis in response to extracellular stimuli in Aspergillus nidulans and Aspergillus fumigatus, Front. Microbiol. 9 (May 2018) 977.
[45] J. Song, N. Li, Y. Xia, Z. Gao, S.F. Zou, Y.H. Yan, S.H. Li, Y. Wang, Y.K. Meng, J.X. Yang, T.G. Kang, Arctigenin confers neuroprotection against mechanical trauma injury in human neuroblastoma SH-SY5Y cells by regulating miRNA-16 and miRNA-199a expression to alleviate inflammation, J. Mol. Neurosci. 60 (1) (Sep 2016) 115–129.
[46] X.T. Li, W. Ma, X.B. Wang, Z. Liang, J.W. Yang, Y. He, Y.F. Dai, T. Zhang, J.W. Wang, K.P. Liu, X.P. Wang, X.K. Zhang, C.Y. Li, J.J. Li, H.Y. Tang, Notoginsenoside R1 promotes the growth of neonatal rat cortical neurons via the Wnt/β-catenin signaling pathway, CNS Neurol. Disord. Drug Targets 17 (7) (2018) 547–556.
[47] J. Krishtal, O. Bragina, K. Metsla, P. Palumaa, V. Tõugu, In situ fibrillizing amyloid-beta 1-42 induces neurite degeneration and apoptosis of differentiated SH-SY5Y cells, PLoS One 12 (10) (Oct 2017) e0186636.
[48] J. Ni, Z. Wu, J. Meng, A. Zhu, X. Zhong, S. Wu, H. Nakanishi, The neuroprotective effects of Brazilian green propolis on neurodegenerative damage in human neuronal SH-SY5Y cells, Oxidative Med. Cell. Longev. 8 (33) (2017) 1069–1079.
[49] Y.K. Chen, H.C. Wang, C.T. Ho, H.Y. Chen, S. Li, H.L. Chan, T.W. Chung, K.T. Tan, Y.R. Li, C.C. Lin, 5-Demethylnobiletin promotes the formation of polymerized tubulin, leads to G2/M phase arrest and induces autophagy via JNK activation in human lung cancer cells, J. Nutr. Biochem. 26 (5) (May 2015) 484–504.
[50] M. Chen, L. Jiang, Y. Li, G. Bai, J. Zhao, M. Zhang, J. Zhang, Hydrogen protects against liver injury during CO_2 pneumoperitoneum in rats, Oncotarget 9 (2) (Dec 2018) 2631.
[51] Z. Gao, H. Wang, B. Zhang, X. Wu, Y. Zhang, P. Ge, G. Chi, J. Liang, Trehalose inhibits H_2O_2-induced autophagic death in dopaminergic SH-SY5Y cells via mitigation of ROS-dependent endoplasmic reticulum stress and AMPK activation, Int. J. Med. Sci. 15 (10) (Jun 2018) 1014–1024.
[52] J. Liang, D. Kulasiri, S. Samarasinghe, Computational investigation of amyloid-β-induced location- and subunit-specific disturbances of NMDAR at hippocampal dendritic spine in Alzheimer's disease, PLoS One 12 (8) (Aug 2017) e0182743.
[53] K.A. Krogh, N. Wydeven, K. Wickman, S.A. Thayer, HIV-1 protein Tat produces biphasic changes in NMDA-evoked increases in intracellular Ca^{2+} concentration via activation of Src kinase and nitric oxide signaling pathways, J. Neurochem. 130 (5) (Sep 2014) 642–656.
[54] H. Ai, W. Lu, M. Ye, W. Yang, Synaptic non-GluN2B-containing NMDA receptors regulate tyrosine phosphorylation of GluN2B 1472 tyrosine site in rat brain slices, Neurosci. Bull. 29 (5) (Sep 2013) 614–620.
[55] J.J.P. Palop, J. Chin, E.D. Roberson, J. Wang, M.T. Thwin, N. Bien-Ly, J. Yoo, K.O. Ho, G.Q. Yu, A. Kreitzer, S. Finkbeiner, J.L. Noebels, Aberrant excitatory neuronal activity and compensatory remodeling of inhibitory hippocampal circuits in mouse models of Alzheimer's disease, Neuron 55 (5) (Sep 2007) 697–711.
[56] J. Chin, J.J. Palop, J. Puoliväli, C. Massaro, N. Bien-Ly, H. Gerstein, K. Scearce-Levie, E. Masliah, L. Mucke, Fyn kinase induces synaptic and cognitive impairments in a transgenic mouse model of Alzheimer's disease, J. Neurosci. 25 (42) (Oct 2005) 9694–9703.
[57] S.W. Fowler, A.C. Chiang, R.R. Savjani, M.E. Larson, M.A. Sherman, D.R. Schuler, J.R. Cirrito, S.E. Lesné, J.L. Jankowsky, Genetic modulation of soluble Aβ rescues cognitive and synaptic impairment in a mouse model of Alzheimer's disease, J. Neurosci. 34 (23) (Jun 2014) 7871–7885.
[58] J.W. Um, S.M. Strittmatter, Amyloid-β induced signaling by cellular prion protein and Fyn kinase in Alzheimer disease, Prion 7 (1) (Feb 2013) 37–41.
[59] J. Zhu, Y. Liang, S. Yue, G. Fan, H. Zhang, M. Zhang, Combination of Panaxadiol and Panaxatriol type Saponins and Ophioponins from Shenmai formula attenuates lipopolysaccharide-induced inflammatory injury in cardiac microvascular endothelial cells by blocking NF-kappa B pathway, J. Cardiovasc. Pharmacol. 69 (3) (Mar 2017) 140–146.